RAA 2016 Vol. **16** No. **8**, 120 (8pp) doi: 10.1088/1674–4527/16/8/120
http://www.raa-journal.org *http://iopscience.iop.org/raa*

***R**esearch in*
***A**stronomy and*
***A**strophysics*

Asteroseismology of the DBV star CBS 114

Yan-Hui Chen

Institute of Astrophysics, Chuxiong Normal University, Chuxiong 675000, China; *yanhuichen1987@ynao.ac.cn*
School of Physics and Electronical Science, Chuxiong Normal University, Chuxiong 675000, China
Key Laboratory for the Structure and Evolution of Celestial Objects, Chinese Academy of Sciences, Kunming 650011, China

Received 2015 October 31; accepted 2016 April 1

Abstract Asteroseismology is a unique and powerful tool to investigate the internal structure of stars. CBS 114 is the sixth known pulsating DBV star. It was observed by Handler, Metcalfe, & Wood at the South African Astronomical Observatory over three weeks in 2001. Then, it was observed by Metcalfe et al. for seven nights (2004 Feb. 19–25) on the 1.8 m telescope at the Bohyunsan Optical Astronomy Observatory and seven nights (2004 Feb. 21–27) on the 2.1 m telescope at the McDonald Observatory. Totally two triplets, four doublets, and five singlets were identified. The frequency splitting values are very different, from 5.2 μHz to 11.9 μHz, which may reflect differential rotations. We evolve grids of white dwarf models by `MESA`. Cores, added with He/C envelopes, of those white dwarf models are inserted into `WDEC` to evolve grids of DBV star models. With those DBV star models, we calculate eigenperiods. Those calculated periods are used to fit observed periods. A best-fitting model is selected. The parameters are $T_{\rm eff} = 25\,000$ K, $M_* = 0.740\ M_\odot$ and $\log(M_{\rm He}/M_*) = -4.5$. With the relatively large stellar mass, the effective temperature is close to the previous spectroscopic result. In addition, kinetic energy distributions are calculated for the best-fitting model. We find that the observed modes with large frequency splitting values are fitted by the calculated modes with a large amount of kinetic energy distributed in the C/O core. After preliminary analysis, we suggest that the C/O core may rotate at least two times faster than the helium layer for CBS 114.

Key words: stars: oscillations (including pulsations) — stars: individual (CBS 114) — white dwarfs

1 INTRODUCTION

White dwarfs are the final evolutionary stage of about 98% of stars (Fontaine et al. 2001). Research on white dwarfs is significant in many fields. About 80% of white dwarfs show a hydrogen atmosphere (DA type) and about 20% of them show a helium atmosphere (DB type) (Bischoff-Kim & Metcalfe 2011).

Basically, there are no thermonuclear reactions occurring in white dwarfs. They are cooling down by eradiation. Along the cooling track, there are instability strips corresponding to DOVs (around 75 000 K to 170 000 K), DBVs (around 22 000 K to 29 000 K) and DAVs (around 10 800 K to 12 270 K) (Winget & Kepler 2008). The pulsation of white dwarfs makes it possible for us to study their internal structure.

Observed eigenfrequencies carry information about the internal structure of a pulsating star. Asteroseismology can be used to detect this type of information about the internal structure. White dwarfs are g-mode pulsators. Radial order k, spherical harmonic degree l and azimuthal number m are used to characterize an eigenmode. Tassoul (1980) published an asymptotic theory for g-modes described by

$$\Delta\bar{\rm P}(l) = \frac{2\pi^2}{\sqrt{l(l+1)}\int_0^R \frac{|N|}{r}dr}. \quad (1)$$

In Equation (1), R is stellar radius. The Brunt-Väisälä frequency N should be calculated as an absolute value. The parameter k cannot be identified from observations. It shows the nodes of the standing wave inside a star. According to Equation (1), relative radial orders may be counted from observations. Star rotation can cause the phenomenon of frequency splitting. An approximate formula that describes the relationship between frequency splitting ($\delta\nu_{k,l}$) and rotational period ($P_{\rm rot}$) was reported by Brickhill (1975) as

$$\begin{aligned} m\delta\nu_{k,l} &= \nu_{k,l,m} - \nu_{k,l,0} \\ &= \frac{m}{P_{\rm rot}}\left[1 - \frac{1}{l(l+1)}\right]. \end{aligned} \quad (2)$$

In Equation (2), the parameter m is taken to be an integer from $-l$ to l. For $l = 1$, modes with $m = -1, 0, +1$ form

a triplet. For $l = 2$, modes with $m = -2, -1, 0, +1, +2$ form a quintuplet. According to Equation (2), the faster a star rotates, the larger the frequency splits. The frequency splitting can be used to study the phenomenon of star rotation. The values of different frequency splittings can be used to study differential rotation. Assuming low k modes are more sensitive to the interior than high k modes, Winget et al. (1994) reported that the envelope of GD 358 rotated some 1.8 times faster than its core. Studying rotational splitting inversions of observational data for GD 358, Kawaler et al. (1999) reported that the core rotated faster than its envelope.

GD 358 is the prototype of the DBV class. DBV stars are considered to be powerful probes of the energy loss rate for plasma neutrinos (Winget et al. 2004). Kim et al. (2006) studied the energy loss rate for plasma neutrinos by measuring the rate of change for the period of hot DBV stars. In addition, research on DBV stars is helpful to check the theory of stellar evolution. Dehner & Kawaler (1995) tried to study evolutionary connections between PG 1159 stars and DBV stars. Diffusion has an important effect on the evolutions. The evolutionary scenario requires a Very Late Thermal Pulse (VLTP) burning off the residual hydrogen in the envelope during post-asymptotic giant branch (post-AGB) evolution. Iben et al. (1983) reported that about 20% of post-AGB stars would experience a VLTP when they descend to the white dwarf cooling track. However, it is difficult to interpret the origin of the 'DB gap' (Liebert et al. 1986). After the VLTP process, little hydrogen ($\log(M_{\rm H}/M_*) \sim -11$) is left (Herwig et al. 1999). When the effective temperature cools to 30 000 K, helium convection dilutes the hydrogen that is left in the photosphere. This helium convection may be interpreted in terms of the 'DB gap'. Hence, asteroseismological study of DBV stars is significant and meaningful.

CBS 114 is the sixth known DBV star discovered by Winget & Claver (1988, 1989). Handler et al. (2002) (HMW2002) described their 65 h of single-site time-resolved CCD photometry targeting CBS 114. Totally, seven independent modes were identified. Some of them might need corrections of daily alias 11.60 μHz, as they reported. Taking a C-core, O-core and C/O-core into account, they conducted an asteroseismological study of those seven independent modes (assuming $l = 1$). In order to obtain more modes to constrain fitting models for CBS 114, a dual-site campaign using 2 m class telescopes was organized by Metcalfe et al. (2005) in February 2004. The previous seven modes were recovered and four new ones were discovered. With a pure carbon core and uniform He/C envelope, Metcalfe et al. (2005) made grids of white dwarf models to fit those 11 $l = 1$ modes. The identified components show different frequency splitting values, from 5.2 μHz to 11.9 μHz, which may correspond to the phenomenon of differential rotation.

Paxton et al. (2011) published a description of Modules for Experiments in Stellar Astrophysics (MESA), which can evolve stars from the pre-main sequence to the white dwarf stage. We try to insert the core and envelope compositions of white dwarf models evolved by MESA into an early program, the White Dwarf Evolution Code (WDEC) (Wood 1990). With this method, grids of DBV star models are evolved with an element diffusion effect. We conduct an asteroseismological study of CBS 114 and try to study its differential rotation.

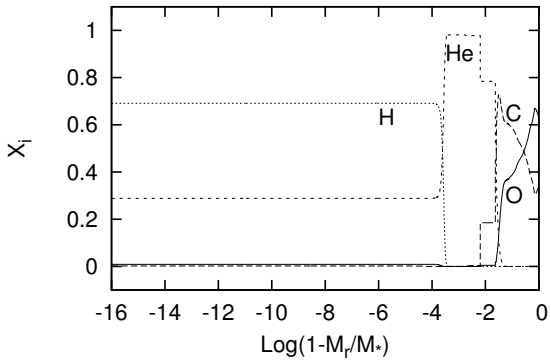

Fig. 1 Abundance of a 0.614 $M_\odot$ white dwarf model evolved from a 2.8 $M_\odot$ main sequence star.

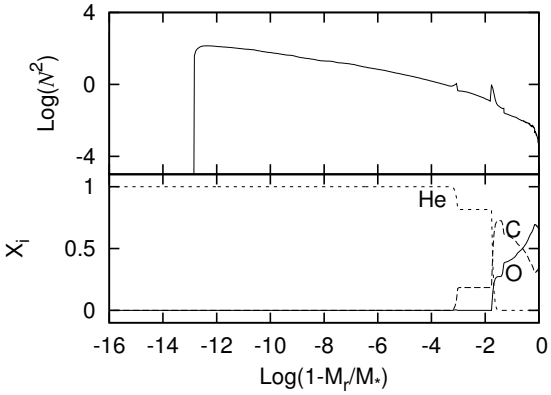

Fig. 2 Diagram of abundance and Brunt-Väisälä frequency for a DBV star. The model parameters are $T_{\rm eff} = 25\,000$ K, $M_* = 0.600\ M_\odot$ and $\log(M_{\rm He}/M_*) = -3.0$.

In Section 2, we introduce the input physics and model calculations. Model fittings on CBS 114 are shown in Section 3. In Sections 3.1, 3.2 and 3.3, we study mode identifications, fitting results and differential rotations associated with CBS 114 respectively. Finally, we provide some discussions and summarize our conclusions in Section 4.

2 INPUT PHYSICS AND MODEL CALCULATIONS

MESA is a new program to simulate star evolutions, which can evolve stars from the pre-main sequence stage to the white dwarf stage. The cores of white dwarfs evolved by MESA are results of thermonuclear burning. The opacities are from Cassisi et al. (2007). The thermonuclear reaction

Table 1 Information about calculated models. In the header, MS, WD(MESA) and WD(WDEC) respectively denote stellar mass of main sequence stars, white dwarfs evolved by MESA and white dwarfs evolved by WDEC. $M_{\rm core}$(MESA) is the core mass of a white dwarf evolved by MESA. $M_{\rm en}$ is the He/C envelope mass. In the envelope, $X_{\rm C(en)}$ and $X_{\rm He(en)}$ denote the abundance of carbon and helium respectively.

MS ($M_\odot$) (1)	WD(MESA) ($M_\odot$) (2)	$M_{\rm core}$(MESA) ($M_\odot$) (3)	WD(WDEC) ($M_\odot$) (4)	$\log(M_{\rm en}/M_{\rm core})(X_{\rm C(en)}, X_{\rm He(en)})$ (5)
2.0	0.580	0.558	0.550–0.575	–1.714 (0.155, 0.845)
2.8	0.614	0.595	0.580–0.605	–1.754 (0.185, 0.815)
3.0	0.633	0.616	0.610–0.635	–1.938 (0.171, 0.829)
3.2	0.659	0.644	0.640–0.665	–2.085 (0.145, 0.855)
3.4	0.689	0.675	0.670–0.695	–1.844 (0.138, 0.862)
3.6	0.723	0.713	0.700–0.725	–2.328 (0.046, 0.954)
3.8	0.751	0.742	0.730–0.755	
4.0	0.782	0.774	0.760–0.785	–2.430 (0.025, 0.975)
4.5	0.805	0.799	0.790–0.815	–2.592 (0.055, 0.945)
5.0	0.832	0.827	0.820–0.850	

rates are from Caughlan & Fowler (1988) and Angulo et al. (1999), see Paxton et al. (2011) for more details. We downloaded and installed the 4298 version of MESA. A module named 'make_co_wd' (mesa/star/test_suite/make_co_wd) was used to evolve stars from the main sequence stage to the white dwarf stage. With default input settings (mixing length parameter $\alpha = 2.0$ and metal abundance $Z = 0.02$), we evolved stellar mass for main sequence stars from 2.0 $M_\odot$ to 5.0 $M_\odot$, as shown in the first column in Table 1. On the Hertzsprung-Russell diagram, we can trace their luminosity over the course of the evolution. When those stars enter the white dwarf cooling track, we stop their evolutions. The corresponding white dwarf masses are shown in the second column in Table 1. Those white dwarf models evolved with 'make_co_wd' usually have a thick helium layer and hydrogen atmosphere.

In Figure 1, we plot the abundance of a 0.614 $M_\odot$ white dwarf model which evolved from a 2.8 $M_\odot$ main sequence star. We remove the C/O core ($M_{\rm core} = 0.595\ M_\odot$). With this method, those core masses are listed in the third column in Table 1.

In Figure 1, we can see that there is an He/C envelope above the C/O core. We take the location where the He abundance is 0.5 as being the boundary of envelope/core. We define $M_{\rm en}$ as the mass of the He/C envelope. Log($M_{\rm en}/M_{\rm core}$) equals –1.754 for the model in Figure 1. In the envelope, $X_{\rm C(en)}$ is defined as carbon abundance and $X_{\rm He(en)}$ is helium abundance.

In Figure 1, $X_{\rm C(en)}$ equals 0.185 and $X_{\rm He(en)}$ equals 0.785. The other 3% are abundances of ^{16}O, ^{18}O, ^{20}Ne, ^{22}Ne, ^{24}Mg and ^{28}Si. For the helium layer in Figure 1, we can also see that the He abundance is a little smaller than 1.000. However, we only calculate ^{1}H(H), ^{4}He(He), ^{12}C(C) and ^{16}O(O) by WDEC. For approximate calculations, we take $X_{\rm C(en)} = 0.185$ and $X_{\rm He(en)} = 0.815$ for the model, as shown in the fifth column of Table 1.

WDEC is a historical program to simulate white dwarf evolutions, which is convenient to evolve grids of white dwarf models. The cores of white dwarfs evolved by WDEC are artificially constructed previously, such as full C, full O, homogeneous C/O profiles and so on. Therefore, we try to insert the core profiles of white dwarfs calculated by MESA into WDEC to evolve grids of white dwarf models. The equation of state is from Lamb (1974) and Saumon et al. (1995). The radiative opacities and conductive opacities are from Itoh et al. (1983). The mixing length theory is from Bohm & Cassinelli (1971) and Tassoul et al. (1990). The ratio of mixing length to pressure scale height (α), for a DBV star, is usually adopted around 1.25 (Bergeron et al. 2011; Montgomery 2007; Koester 2010). We adopt $\alpha = 1.25$ for calculations.

With MESA evolutions, we obtain a grid of white dwarf models. The core mass, corresponding envelope mass, carbon abundance and approximate helium abundance are shown in Table 1. Each core is used to evolve a group of white dwarfs by WDEC. For example, the 0.595 $M_\odot$ core is used to evolve white dwarfs from 0.580 $M_\odot$ to 0.605 $M_\odot$. The mass range of white dwarf models evolved by WDEC is shown in the fourth column of Table 1.

After MESA evolutions, we take out the structure parameters, including mass, radius, luminosity, pressure, temperature, entropy and carbon abundance. Those parameters are inserted into the prototype models in WDEC. The oxygen abundance approximately equals 1.000 minus the carbon abundance. The envelope masses as well as C and He abundances in the envelope are constrained by the last column in Table 1. The envelope masses are different in Table 1. There is no envelope for white dwarfs evolved from 3.8 $M_\odot$ or 5.0 $M_\odot$ main sequence stars. Core compositions and envelope abundances of white dwarfs evolved by MESA are used as input physics for WDEC. WDEC evolves white dwarfs from above 100 000 K to the DBV instability strip. A process describing element diffusion derived by Thoul et al. (1994) is incorporated into WDEC by Su et al. (2014). We take 500 000 years as the evolution step.

Grids of white dwarf models are evolved by WDEC. The stellar mass M_* is from 0.550 $M_\odot$ to 0.850 $M_\odot$ in steps of 0.005 $M_\odot$. The effective temperature is from 21 000 K to 30 000 K in steps of 200 K. The envelope

mass fraction is shown in the last column of Table 1 for each group of white dwarfs. The helium layer mass fraction ($\log(M_{\rm He}/M_*)$) is from –6.0 to –3.0 in steps of 0.5.

In Figure 2, we show a diagram of abundance and Brunt-Väisälä frequency for an evolved DBV star. The model parameters are $T_{\rm eff} = 25\,000$ K, $M_* = 0.600\ M_\odot$ and $\log(M_{\rm He}/M_*) = -3.0$. Its core compositions and envelope abundances are evolved from the white dwarf model in Figure 1. The composition gradients in the lower panel of Figure 2 cause 'spikes' in the upper panel. Those 'spikes' may cause a mode trapping effect (Winget et al. 1981; Brassard et al. 1992). In addition, there is an extremely thin convection zone on the surface of the star. With those grids of DBV star models, we numerically solve the full equations of linear and adiabatic oscillation. Each eigenmode will be scanned out. Those calculated modes will be used to fit the observed modes of CBS 114.

3 MODEL FITTINGS ON CBS 114

In this section, we analyze the previously observed modes for CBS 114 and then apply model fittings to CBS 114. According to different frequency splitting values and distributions of kinetic energy for corresponding fitting modes, we try to study the differential rotation effect for CBS 114.

3.1 Mode Identifications for CBS 114

In Table 2, we show mode identifications for CBS 114 by HMW2002 and Metcalfe et al. (2005). HMW2002 identified seven independent modes. They were recovered by mode identifications of Metcalfe et al. (2005). In the second column, $Fre.$ denotes the frequencies identified by Metcalfe et al. (2005). In the parentheses, $Fre.$ in HMW denotes the frequencies identified by HMW2002. The minus sign means that the negative daily alias (f_i − 11.60 μHz) may also be the correct eigenfrequency. The plus sign means that the positive daily alias (f_i + 11.60 μHz) may also be the correct eigenfrequency, as reported in Table 2 of HMW2002. Amp2001 is the amplitude of modes identified by HMW2002. Amp1998 is the amplitude of modes re-analyzed by HMW2002 based on the observations of Winget & Claver (1988, 1989). Metcalfe et al. (2005) treated f_{10} + 11.60 μHz as the eigenmode. In addition to those seven modes, Metcalfe et al. (2005) also identified four new ones, f_1, f_2, f_3 and f_9.

Metcalfe et al. (2005) identified two triplets (f_4, f_5) and two doublets (f_9, f_{11}), as shown in Table 2. In addition, we also treat modes f_7 and f_8 as doublets, which are identified by both HMW2002 and Metcalfe et al. (2005). The frequency splitting value is shown in the third column in Table 2. The mode f_7 identified by HMW2002 may be three values, 1824.04 μHz, 1835.64 μHz and 1847.24 μHz. Therefore, the frequency splitting for f_7 may be 5.56 μHz, 6.04 μHz and 17.64 μHz. Those frequency splitting values in Table 2 are scattered, which is very important for the study of differential rotation.

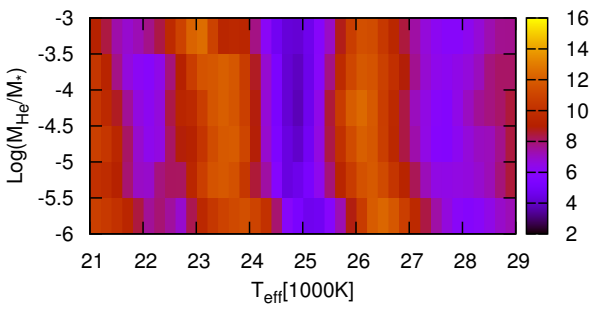

Fig. 3 Color residual diagram for models of $M_* = 0.740\ M_\odot$. The ordinate denotes the helium layer mass. The abscissa denotes the effective temperature. The color denotes the residual. The bluer the color, the smaller the residual.

In the fifth column in Table 2, we can see that the amplitudes of f_4, f_6 and f_8 are decreasing from 2001 to 2004. This phenomenon has also been observed in other cases, such as the DBV star GD 358 (Kepler et al. 2003). It may be caused by a convective driving mechanism (Dupret et al. 2008). In the sixth column, we show an l identification. If triplets or doublets are observed, the modes will be identified as $l = 1$. There are $l = 2$ modes observed on the prototype DBV GD 358 (Kepler et al. 2003) and on the DBV KIC 8626021 (Bischoff-Kim et al. 2014) identified from *Kepler* observations. We assume they are $l = 1$ or 2 modes. The $l \geq 3$ modes suffer from significant geometric cancelation (Dziembowski 1977).

Since the modes identified by Metcalfe et al. (2005) recover the seven previously identified independent modes, we use these modes to constrain fitting models. For two triplets, we can see that the $m = 0$ modes have higher amplitudes. Therefore, we assume that the singlets are $m = 0$ modes. The higher amplitude modes for doublets are $m = 0$ modes. Finally, there are six $l = 1$, $m = 0$ modes and five $l = 1$ or 2, $m = 0$ modes identified in Table 2. In total, 11 modes are used to constrain fitting models.

3.2 Fitting Results for CBS 114

We use the grids of DBV star models to fit the 11 identified $m = 0$ modes. A formula for fitting the residuals is expressed as

$$\sigma_{\rm RMS} = \sqrt{\frac{\sum_1^{n_{\rm obs}} (\mathrm{Per.}_{\rm mod} - \mathrm{Per.}_{\rm obs})^2}{n_{\rm obs}}}. \qquad (3)$$

In Equation (3), $n_{\rm obs}$ is the number of observed modes. In this paper, $n_{\rm obs}$ is 11. $\mathrm{Per.}_{\rm mod}$ is the calculated periods and $\mathrm{Per.}_{\rm obs}$ is the observed periods. The model with the smallest $\sigma_{\rm RMS}$ is considered to be the best-fitting one.

In Figure 3, we show the color residual diagram for the fitting results. The bluer the color, the smaller the residual. The smallest $\sigma_{\rm RMS}$ is 2.65 s which corresponds to the best-fitting model. The model parameters are $T_{\rm eff} = 25\,000$ K,

Table 2 Mode identifications by HMW2002 and Metcalfe et al. (2005). Fre. denotes the pulsating frequency in μHz. Per. is the corresponding period in second (s). Fre. Spl. is the frequency splitting value.

ID	Fre. (Fre. in HMW) (μHz)	Fre. Spl. (μHz)	Per. (Per. in HMW) (s)	Amp (Amp2001) (Amp1988) (mmag)	l	m
f_1	1189.9		840.38	3.1	1 or 2	0?
f_2	1252.4		798.46	4.3	1 or 2	0?
f_3	1383.0		723.06	3.0	1 or 2	0?
f_4	1509.0		662.67	7.5	1	-1
		9.8				
f_4	1518.8 (1518.75$^-$)		658.44 (658.43)	11.8 (16–33) (33)	1	0
		11.9				
f_4	1530.7		653.30	9.0	1	$+1$
f_5	1601.2		624.55	4.4	1	-1
		10.9				
f_5	1612.1 (1613.12)		620.31 (619.91)	15.4 (10–17) (15)	1	0
		10.6				
f_5	1622.7		616.27	13.3	1	$+1$
f_6	1729.8 (1729.73)		578.09 (578.13)	7.0 (22–37) (18)	1 or 2	0?
f_7	1829.6 (1835.64^{+-})	17.64?	546.56 (544.77)	3.0 (<4.2) (13)	1	0?
f_8	1963.2 (1969.60)	6.40	509.37 (507.71)	5.5 (11–17) (<5)	1	0?
f_9	2086.5		479.27	4.8	1	-1?
		7.1				
f_9	2093.6		477.65	4.9	1	0?
f_{10}	2317.7 (2306.38$^+$)		431.45 (433.58)	8.9 (4–12) (13)	1 or 2	0?
f_{11}	2510.0 (2509.89$^-$)		398.41 (398.42)	6.8 (4–10) (9)	1	0?
		5.2				
f_{11}	2515.2		397.59	3.2	1	$+1$?

Table 3 The best-fitting models for asteroseismological study by HMW2002, Metcalfe et al. (2005), us and spectroscopic study by Beauchamp et al. (1999) and Kleinman et al. (2013).

	$T_{\rm eff}$(K)	$\log g$	$M_*/M_\odot$	$\log(M_{\rm He}/M_*)$
HMW2002(C-core)	24 600		0.655	–3.96
HMW2002(O-core)	25 800		0.640	–3.96
HMW2002(C/O core)	21 000		0.730	–6.66
Metcalfe et al.(pure C)	25 800		0.630	–5.96
This paper	25 000	8.287	0.740	–4.5
Beauchamp et al.(no H)	26 200	8.00		
Beauchamp et al.(H)	23 300	7.98		
Kleinman et al.	25 754±368	7.95±0.037		

$M_* = 0.740\ M_\odot$ and $\log(M_{\rm He}/M_*) = -4.5$. The model has a gravitational acceleration of $\log g = 8.287$. In Table 1, we can see that the 0.740 $M_\odot$ white dwarf is from the 3.8 $M_\odot$ main sequence star, which has no He/C envelope.

In Figure 4, we show a diagram of abundance and Brunt-Väisälä frequency for the best-fitting model. In the lower panel, there is a C/O envelope above the C/O core, instead of a He/C envelope.

In Table 3, we show best-fitting models of the asteroseismological study by HMW2002, Metcalfe et al. (2005), us and the spectroscopic study by Beauchamp et al. (1999) and Kleinman et al. (2013). Fitting seven independent modes with C-core and O-core white dwarfs, HMW2002 obtained their similar best-fitting models. The parameters are $T_{\rm eff} = 24\,600$ K, $M_* = 0.655\ M_\odot$, $\log(M_{\rm He}/M_*) = -3.96$ and $T_{\rm eff} = 25\,800$ K, $M_* = 0.640\ M_\odot$, $\log(M_{\rm He}/M_*) = -3.96$ respectively.

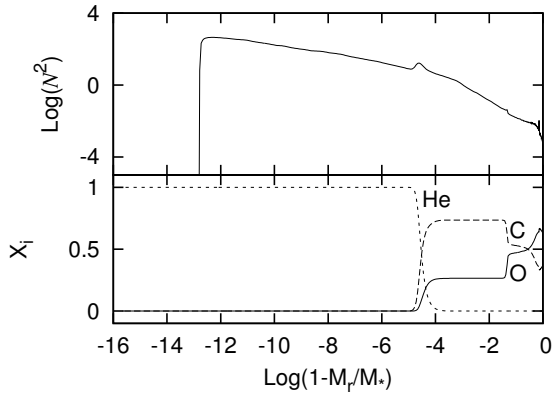

Fig. 4 Diagram of abundance and Brunt-Väisälä frequency for the best-fitting model. The model parameters are $T_{\rm eff} = 25\,000$ K, $M_* = 0.740\ M_\odot$ and $\log(M_{\rm He}/M_*) = -4.5$.

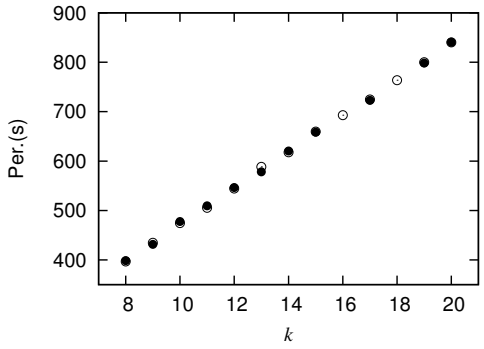

Fig. 5 Diagram of periods versus radial orders. The filled dots are the 11 identified eigenperiods. The open dots are the calculated $l = 1$ modes for the best-fitting model. The radial order is from 8 to 20 for the calculated modes, which can be used as relative radial orders for the observed modes.

Moreover, with C/O core white dwarfs, they obtained a best-fitting model of low effective temperature (21 000 K), large stellar mass (0.730 $M_\odot$) and a thin helium atmosphere ($\log(M_{\rm He}/M_*) = -6.66$). Fitting 11 independent modes with pure carbon core white dwarfs, Metcalfe et al. (2005) obtained a best-fitting model of $T_{\rm eff} = 25\,800$ K, $M_* = 0.630\ M_\odot$ and $\log(M_{\rm He}/M_*) = -5.96$. For spectroscopic work, Beauchamp et al. (1999) obtained a best no hydrogen model of $T_{\rm eff} = 26\,200$ K, $\log g = 8.00$ and an undetectable hydrogen model with $T_{\rm eff} = 23\,300$ K, $\log g = 7.98$. In addition, from the spectroscopic catalog of the Sloan Digital Sky Survey (SDSS) Data Release 7 (DR7), Kleinman et al. (2013) obtained a best-fitting model of $T_{\rm eff} = 25\,754 \pm 368$ K, $\log g = 7.95 \pm 0.037$.

The effective temperature for our best-fitting model is 25 000 K. It is close to the previous asteroseismological results of 24 600 K, 25 800 K and the previous spectroscopic result of 25 754±368 K. The stellar mass for our best-fitting model is 0.740 $M_\odot$. It is obviously more massive than previous results of pure C-core or pure O-core white dwarf fittings. The stellar mass 0.740 $M_\odot$ is close to 0.730 $M_\odot$. Both of them are from C/O core white dwarf fittings to CBS 114. However, the gravitational acceleration ($\log g = 8.287$) for our best-fitting model is obviously larger than the previous spectroscopic results, as shown in Table 3.

3.3 Differential Rotations for CBS 114

In Table 4, we show observed periods, calculated periods, fitting errors and percentage of kinetic energy distributions. The percentage of kinetic energy distributed in the C/O core and He layer is calculated by the equation

$$\frac{{\rm Kin_{core}}}{{\rm Kin_{He}}} = \frac{4\pi \int_0^{R_{\rm He/C}} [(|\tilde{\xi}_{\rm r}(r)|^2 + l(l+1)|\tilde{\xi}_{\rm h}(r)|^2)]\rho_0 r^2 dr}{4\pi \int_{R_{\rm He/C}}^{R} [(|\tilde{\xi}_{\rm r}(r)|^2 + l(l+1)|\tilde{\xi}_{\rm h}(r)|^2)]\rho_0 r^2 dr}. \quad (4)$$

In Equation (4), ρ_0 is the local density and $R_{\rm He/C}$ is the location of the He/C interface. For the best-fitting model, $R_{\rm He/C}$ is located at $\log(1-M_{\rm r}/M_*) = -4.5$. $\tilde{\xi}_{\rm r}(r)$ is the radial displacement and $\tilde{\xi}_{\rm h}(r)$ is the horizontal displacement. The 11 observed modes are fitted by nine $l = 1$ modes and two $l = 2$ modes. The mode f_{10} is fitted by 432.710 s ($l = 2$, $k = 17$) in Table 4, which can also be fitted by the $l = 1$ mode 434.502 s ($l = 1$, $k = 9$) with a small fitting error. However, the mode of f_6 can only be fitted by an $l = 2$ mode. Even when fitted by an $l = 2$ mode, the fitting error is also not small (–5.477 s). We doubt whether f_6 is an $m = 0$ component.

Assuming those 11 modes to be $l = 1$ and $m = 0$, Metcalfe et al. (2005) obtained their best-fitting model with $\sigma_{\rm RMS} = 2.33$ s. They did not show detailed calculated modes or fitting errors. We do not know their fitting result for f_6. For those 11 modes, there is a good mean period spacing of 36.534 s. HMW2002 showed a mean period spacing of 37.1±0.7 s.

In Figure 5, the filled dots show the observed 11 modes. They present a good straight line versus the calculated radial orders. The open dots show the calculated $l = 1$ modes of the best-fitting model. On the whole, the open dots match the filled dots well. In detail, f_6 is badly fitted. However, it is impossible to rule out an $l = 2$ mode in the $l = 1$ sequence. It is also impossible to rule out that f_6 is an $m \neq 0$ mode. Therefore, a relatively reliable identification of f_6 requires more observations.

The percentage of kinetic energy distributions for $l = 1$ modes is shown in the fourth column in Table 4. In the parenthesis of the second column, the frequency splitting values are displayed again. We notice that the observed mode f_{11} with a frequency splitting of 5.2 μHz corresponds to the calculated $l = 1$, $m = 8$ mode. This mode has 56% of the kinetic energy distributed in the He layer. The observed mode f_8 with a frequency splitting of 6.40 μHz corresponds to the calculated $l = 1$, $m = 11$ mode. This mode has 48% of the kinetic energy distributed

Table 4 Table of fitting results. $\mathrm{Per.}_{\mathrm{obs}}$ and $\mathrm{Per.}_{\mathrm{mod}}(l,k)$ denote observed periods and calculated periods respectively. $\mathrm{Kin}_{\mathrm{core}}$ and $\mathrm{Kin}_{\mathrm{He}}$ denote percentage of kinetic energy distributed in the C/O core and He layer for calculated modes respectively.

ID	$\mathrm{Per.}_{\mathrm{obs}}$(Fre. Spl.) (s) (μHz)	$\mathrm{Per.}_{\mathrm{mod}}(l,\,k)$ (s)	($\mathrm{Kin}_{\mathrm{core}}$, $\mathrm{Kin}_{\mathrm{He}}$)	$\mathrm{Per.}_{\mathrm{obs}}-\mathrm{Per.}_{\mathrm{mod}}(l,k)$ (s)
(1)	(2)	(3)	(4)	(5)
f_{11}	398.41 (5.2)	396.681 (1, 8)	(44%, 56%)	1.729
f_{10}	431.45	432.710 (2, 17)		–1.260
		434.502 (1, 9)	(78%, 22%)	
f_9	477.65 (7.1)	474.397 (1, 10)	(66%, 34%)	3.253
f_8	509.37 (6.40)	505.517 (1, 11)	(52%, 48%)	3.867
f_7	546.56 (17.64?)	544.374 (1, 12)	(74%, 26%)	2.186
f_6	578.09	583.567 (2, 24)		–5.477
		588.187 (1, 13)	(48%, 52%)	
f_5	620.31 (10.6,10.9)	617.807 (1, 14)	(67%, 33%)	2.503
f_4	658.44 (11.9, 9.8)	659.540 (1, 15)	(68%, 32%)	–1.100
		692.760 (1, 16)	(62%, 38%)	
f_3	723.06	724.714 (1, 17)	(76%, 24%)	–1.654
		763.581 (1, 18)	(67%, 33%)	
f_2	798.46	800.004 (1, 19)	(60%, 40%)	–1.544
f_1	840.38	840.123 (1, 20)	(73%, 27%)	0.257

in the He layer. In addition, f_4 with frequency splittings of 11.9 μHz and 9.8 μHz correspond to mode $l = 1$, $m = 15$. This mode has 32% of the kinetic energy distributed in the He layer. It seems that the smaller the frequency splitting value for an observed mode, the more kinetic energy is distributed in the He layer for a calculated mode. The phenomenon may be caused by modes partly trapped in the He layer or C/O core. Rotation can cause the frequency splitting effect, as shown in Equation (2). Therefore, we suggest that the C/O core may rotate faster than the He layer for CBS 114. This is a preliminary inference. The frequency splitting values are scattered, being 5.2, 6.40, 7.1, 9.8, 10.6, 10.9 and 11.9 μHz. The frequency splitting values and the kinetic energy distributions show that the C/O core may rotate at least 2 ((11.9, 9.8, 10.6, 10.9)/5.2 ∼2) times faster than the He layer. Kawaler et al. (1999) reported that the center rotated faster than the surface for PG 1159 and the inner core might rotate rapidly for GD358. More observations are required in order to quantify the differential rotation. In addition, the mode f_7 is identified as 1829.6 μHz by Metcalfe et al. (2005) and 1835.64^{+-} by HMW2002. For the calculated mode, only 26% of the kinetic energy is distributed in the He layer. The frequency splitting value may be larger than 11.9 μHz for f_7. Therefore, we suggest that $1835.64 + 11.60$ μHz may be the eigenfrequency and the corresponding frequency splitting value may be 17.64 μHz.

4 DISCUSSION AND CONCLUSIONS

In this paper, we evolve grids of white dwarf models by MESA and then we insert those white dwarf cores into WDEC. This method has been used by us to evolve grids of DAV star models to study EC14012–1446 (Chen & Li 2014). For DBV stars, we improve the method by extracting the He/C envelope from white dwarf models evolved by MESA. Metcalfe et al. (2005) made dual-site observations of CBS 114 and identified 11 independent modes. The $m = 0$ modes in two triplets show higher amplitudes. Therefore, the higher amplitude modes in doublets are identified as $m = 0$ modes. The singlets are identified as $m = 0$ modes. Triplets and doublets are identified as $l = 1$ and singlets are identified as $l = 1$ or 2 by us.

Fitting the 11 identified modes, we obtain a best-fitting model of $T_{\mathrm{eff}} = 25\,000$ K, $M_* = 0.740\ M_\odot$ and $\log(M_{\mathrm{He}}/M_*) = -4.5$. The residual is 2.65 s and the gravitational acceleration is $\log g = 8.287$. The effective temperature is close to the previous spectroscopic result of 25 754±368 K. However, the gravitational acceleration is obviously larger than the spectroscopic result of 7.95±0.037. In fact, our evolved DBV star models are contradictory to the 'DB gap' phenomenon. In future work, we will try to evolve DBV star models with a little hydrogen left in order to pass the 'DB gap'. The effect of convective helium dilution will change those DA stars into DB stars when T_{eff} cools to 30 000 K, as discussed in the Introduction. Kleinman et al. (2004) reported that there was a relative overabundance of DA stars inside the 'DB gap' according to SDSS DR1. The DBV star models with a thin hydrogen atmosphere may have a chance to solve the problem of large gravitational acceleration.

Finally, we study the frequency splitting values for observed modes and the kinetic energy distributions for best-fitting modes. The observed modes with large frequency splitting values correspond to the calculated modes with a large amount of kinetic energy distributed in the C/O core. The frequency splitting values of f_4 and f_5 are basically two times that of f_{11}, as shown in Table 4. We suggest that the C/O core may rotate at least two times faster than the He layer for CBS 114.

Acknowledgements This work is supported by the National Natural Science Foundation of China (Grant No. 11563001), the Research Fund of Chuxiong Normal University (XJGG1501), the Collaborating Research Program of Key Laboratory for the Structure and Evolution of Celestial Objects, Chinese Academy of Sciences (OP201502) and the Yunnan Applied Basic Research Project (2015FD044).

References

Angulo, C., Arnould, M., Rayet, M., et al. 1999, Nuclear Physics A, 656, 3
Beauchamp, A., Wesemael, F., Bergeron, P., et al. 1999, ApJ, 516, 887
Bergeron, P., Wesemael, F., Dufour, P., et al. 2011, ApJ, 737, 28
Bischoff-Kim, A., & Metcalfe, T. S. 2011, MNRAS, 414, 404
Bischoff-Kim, A., Østensen, R. H., Hermes, J. J., & Provencal, J. L. 2014, ApJ, 794, 39
Bohm, K. H., & Cassinelli, J. 1971, A&A, 12, 21
Brassard, P., Fontaine, G., Wesemael, F., & Hansen, C. J. 1992, ApJS, 80, 369
Brickhill, A. J. 1975, MNRAS, 170, 405
Cassisi, S., Potekhin, A. Y., Pietrinferni, A., Catelan, M., & Salaris, M. 2007, ApJ, 661, 1094
Caughlan, G. R., & Fowler, W. A. 1988, Atomic Data and Nuclear Data Tables, 40, 283
Chen, Y. H., & Li, Y. 2014, MNRAS, 443, 3477
Dehner, B. T., & Kawaler, S. D. 1995, ApJ, 445, L141
Dupret, M. A., Quirion, P. O., Fontaine, G., Brassard, P., & Grigahcène, A. 2008, Journal of Physics Conference Series, 118, 012051
Dziembowski, W. 1977, Acta Astronomica, 27, 1
Fontaine, G., Brassard, P., & Bergeron, P. 2001, PASP, 113, 409
Handler, G., Metcalfe, T. S., & Wood, M. A. 2002, MNRAS, 335, 698
Herwig, F., Blöcker, T., Langer, N., et al. 1999, A&A, 349, L5
Iben, Jr., I., Kaler, J. B., Truran, J. W., & Renzini, A. 1983, ApJ, 264, 605
Itoh, N., Mitake, S., Iyetomi, H., & Ichimaru, S. 1983, ApJ, 273, 774
Kawaler, S. D., Sekii, T., & Gough, D. 1999, ApJ, 516, 349
Kepler, S. O., Nather, R. E., Winget, D. E., et al. 2003, A&A, 401, 639
Kim, A., Winget, D. E., & Montgomery, M. H. 2006, Mem. Soc. Astron. Italiana, 77, 460
Kleinman, S. J., Harris, H. C., Eisenstein, D. J., et al. 2004, ApJ, 607, 426
Kleinman, S. J., Kepler, S. O., Koester, D., et al. 2013, ApJS, 204, 5
Koester, D. 2010, Mem. Soc. Astron. Italiana, 81, 921
Lamb, Jr., D. Q. 1974, Evolution of Pure Carbon-12 White Dwarfs., PhD Thesis (The University of Rochester)
Liebert, J., Wesemael, F., Hansen, C. J., et al. 1986, ApJ, 309, 241
Metcalfe, T. S., Nather, R. E., Watson, T. K., et al. 2005, A&A, 435, 649
Montgomery, M. H. 2007, Communications in Asteroseismology, 150, 253
Paxton, B., Bildsten, L., Dotter, A., et al. 2011, ApJS, 192, 3
Saumon, D., Chabrier, G., & van Horn, H. M. 1995, ApJS, 99, 713
Su, J., Li, Y., Fu, J.-N., & Li, C. 2014, MNRAS, 437, 2566
Tassoul, M. 1980, ApJS, 43, 469
Tassoul, M., Fontaine, G., & Winget, D. E. 1990, ApJS, 72, 335
Thoul, A. A., Bahcall, J. N., & Loeb, A. 1994, ApJ, 421, 828
Winget, D. E., van Horn, H. M., & Hansen, C. J. 1981, ApJ, 245, L33
Winget, D. E., & Claver, C. F. 1988, IAU Circ., 4595, 3
Winget, D. E., & Claver, C. F. 1989, in Lecture Notes in Physics, Berlin Springer Verlag, 328, IAU Colloq. 114: White Dwarfs, ed. G. Wegner, 290
Winget, D. E., Nather, R. E., Clemens, J. C., et al. 1994, ApJ, 430, 839
Winget, D. E., Sullivan, D. J., Metcalfe, T. S., et al. 2004, ApJ, 602, L109
Winget, D. E., & Kepler, S. O. 2008, ARA&A, 46, 157
Wood, M. A. 1990, Astero-Archaeology: Reading the Galactic History Recorded in the White Dwarf Stars, PhD Thesis (The Univesity of Texas at Austin)